Non-Linear Forced Response of Vibrating Mechanical Systems: The Impact of Computational Parameters

applied sciences

MDPI

Article

Non-Linear Forced Response of Vibrating Mechanical Systems: The Impact of Computational Parameters

Enio Colonna [1,*], Teresa Berruti [1], Daniele Botto [1] and Andrea Bessone [2]

[1] Department of Mechanical and Aerospace Engineering, Polytechnic University of Turin, 10129 Turin, Italy; teresa.berruti@polito.it (T.B.); daniele.botto@polito.it (D.B.)
[2] Mechanical Integrity Group, Ansaldo Energia, 16152 Genova, Italy; andrea.bessone@ansaldoenergia.com
* Correspondence: enio.colonna@polito.it

Abstract

The harmonic balance method (HBM) is a widely used method for determining the forced response of non-linear systems such as bladed disks. This paper focuses on analyzing the sensitivity of this method to key computational parameters and its robustness. HBM and HBM coupled with pseudo arc length continuation are used in this paper to solve the equation of motion of a test case. The pseudo arc length continuation is necessary because when intermittent contact occurs, natural continuation cannot guarantee solver convergence. Intermittent contact, in addition to turning points, introduces further problems, which are caused by an infinite sequence of decaying, but not zero, Fourier coefficients. This results in the need to oversample the non-linear force time signal to avoid convergence problems. The computational parameters investigated in this paper are the samples per period, which determine the number of points in which the time signal is discretized, and the harmonic truncation order. In addition, the connection of contact parameters, such as friction and contact stiffness, with computational parameters is analyzed. This study shows that the number of time samples per period is the most limiting parameter when intermittent contact occurs; whereas, in the absence of intermittent contact convergence, problems can be avoided with a reasonable number of time points. Poor discretization of the signal leads to a bad computation of Fourier coefficients and thus a lack of convergence. Sensitivity analysis shows that the samples per period depend on the contact parameters, especially normal stiffness. To ensure the solver robustness, it is important to set the computation parameters appropriately to ensure the convergence of the solver while avoiding unnecessary computation effort.

Keywords: non-linear forced response; friction contact; intermittent contact; pseudo arc length continuation

Academic Editor: Junhong Park

Received: 27 June 2025
Revised: 8 August 2025
Accepted: 14 August 2025
Published: 19 August 2025

Citation: Colonna, E.; Berruti, T.; Botto, D.; Bessone, A. Non-Linear Forced Response of Vibrating Mechanical Systems: The Impact of Computational Parameters. *Appl. Sci.* **2025**, *15*, 9112. https://doi.org/10.3390/app15169112

1. Introduction

In the field of turbomachinery, it is very important to minimize blade damage due to vibrations, caused by blade–fluid interaction. To this end, mechanical devices that take advantage of dry friction [1–3], such as under-platform dampers, [4–7] and snubbers [8] are usually used to dissipate a part of the kinetic energy during vibratory phenomena. A numerical and experimental comparison of three damper geometries is performed in [9]. In previously cited studies, calculations with dry friction devices were performed, and the effect on the non-linear response of turbine blades was investigated.

The use of these devices helps to increase the fatigue life of the blade, but on the other hand, the presence of friction forces between the contact surfaces introduces non-linearities into the equation of motion of the system. Therefore, it is necessary to adopt computational methods that take such non-linearities into account. The harmonic balance method (HBM) is a method widely used and discussed in the literature [10–13] to determine the forced response of non-linear systems.

In this paper, the HBM was used to solve the equations of motion of the test case presented in Section 3 without considering secondary effects, such as heat generated by friction, as they are not relevant to the purpose of this work.

Although the classical HBM method was used in this paper, it is important to note that there are innovative studies in the literature that optimize this method by improving its convergence [14–16], as well as studies that consider the influence of heat generated by friction on the modal characteristics of the system [17].

The main goal of this paper is to provide guidelines for designers using non-linear computational tools in the field of turbomachinery. This paper focuses on a sensitivity analysis on the parameters that affect the convergence of the non-linear solver. The first parameter investigated is the number of samples per period, then the effect of the harmonic truncation order is discussed and finally the effect of contact parameters is explored. Contact parameters, from the perspective of this paper, are input parameters for the non-linear solver. However, it is important to highlight that they must model the physical properties of the contact. These parameters can be derived from analytical models or from experimental tests on dedicated test rigs. For instance, the normal stiffness, in some cases, can be estimated using Hertz contact theory, which defines relationships between the indentation depth and the normal force for two contacting bodies. The single relationship depends on the elastic modulus, the surface geometry, the Poisson's ratio and the surface finish, and the ratio between the normal force and the indentation depth can be expressed as a normal stiffness, which in a contact model is represented as a spring element. In [18,19] different analytical models and test rigs for contact parameters estimation are presented and discussed. The work presented in [20] compares contact stiffness definitions according to a semi-analytical model with those based on classical tuning using experimental tests.

Several papers address this issue in the literature, but the importance and the criticality of samples per period and harmonic order truncation are extensively discussed in [21], in which the convergence issues due to poor time discretization when AFT-HBM scheme is used are emphasized. The effect of contact parameters on the solver convergence has not been discussed so far.

The main outcome of this paper is the identification of how the different parameters affect the non-linear response calculation, computation times and solver convergence so they can be optimally set to improve the robustness of the tool. This paper is organized as follows.

Section 2 describes the computational method implemented to improve the convergence of the HBM.

Section 3 presents the test case and shows the results of simulations performed with and without intermittent contact.

Section 4 presents a sensitivity analysis and discusses how the calculational parameters affect the convergence of the non-linear solver and the computation time.

Section 5 provides guidelines for designers based on the results of the sensitivity analysis.

2. Computation Methods

The harmonic balance method is a numerical method that can be used for calculating with accuracy and efficiency the steady-state nonlinear dynamic response of a mechanical system. The main assumption underlying this method is the periodicity of the nonlinear term of the equation.

The equation of motion of a turbine blade can be written as follows:

$$[M]\left\{\ddot{X}\right\} + [C]\left\{\dot{X}\right\} + [K]\{X\} = \{F_{Ext}\} - \{F_{NL}\}\left(X, \dot{X}, t\right) \quad (1)$$

The terms of the previous equations are defined below,

- [M], [C], [K] are, respectively, the system mass, viscous damping and stiffness matrices
- $\{F_{Ext}\}$ is the external excitation vector
- $\{F_{NL}\}$ is the nonlinear force vector

In Equation (1) the second forcing term represents the nonlinear force vector, which for turbine applications is usually the friction force acting on the contact nodes, which arises from relative motion of contact surfaces. The presence of the nonlinear term, which is non-harmonic, implies that the solution of this second order differential equation is not harmonic, so it cannot be written as a single frequency term but can be expressed with a Fourier series:

$$\{X(t)\} \cong \overline{X}_0 + \sum_{n=1}^{nh} \{\overline{X}\}^{(n)} e^{in\omega t} \quad (2)$$

The same reasoning can be applied to the nonlinear force term of the equation:

$$\{F_{NL}(t)\} \cong \overline{F}_{NL_0} + \sum_{n=1}^{nh} \{\overline{F}_{NL}\}^{(n)} e^{in\omega t} \quad (3)$$

In Equations (2) and (3):

- $\overline{X}_0, \overline{F}_{NL_0}$ are the displacement and nonlinear force static terms
- $\overline{X}^{(n)}, \overline{F}_{NL}{}^{(n)}$ are the displacement and nonlinear force n-th Fourier coefficient

Neglecting static terms because they will come, for example, from a static analysis and substituting Equations (2) and (3) in Equation (1), leads to

$$-(n\omega)^2[M]\sum_{n=1}^{nh}\{\overline{X}\}^{(n)}e^{in\omega t} + (in\omega)[C]\sum_{n=1}^{nh}\{\overline{X}\}^{(n)}e^{in\omega t} + [K]\sum_{n=1}^{nh}\{\overline{X}\}^{(n)}e^{in\omega t} = \{\overline{F}_{ext}\}e^{i\omega t} - \sum_{n=1}^{nh}\{\overline{F}_{NL}\}^{(n)}e^{in\omega t} \quad (4)$$

Bringing together the common factors at first member of the Equation (4), gives the following equations:

$$\sum_{n=1}^{nh}\left(-(n\omega)^2[M] + in\omega[C] + [K]\right)\{\overline{X}\}^{(n)}e^{in\omega t} = \{\overline{F}_{Ext}\}e^{i\omega t} - \sum_{n=1}^{nh}\{\overline{F}_{NL}\}^{(n)}e^{in\omega t} \quad (5)$$

Equation (5) is a set of coupled equations because the nonlinear force depends on all harmonic components of the displacement that are considered in the calculation. Simplifying the temporal term and defining the dynamic stiffness of the system as

$$[D]^{(n)} = -(n\omega)^2[M] + in\omega[C] + [K] \quad (6)$$

For $n = 1$

$$[D]^{(1)}\{\overline{X}\}^{(1)} = \{\overline{F}_{Ext}\}^{(1)} - \{\overline{F}_{NL}\}^{(1)} \quad (7)$$

For $n > 1$

$$[D]^{(n)}\{\overline{X}\}^{(n)} = -\{\overline{F}_{NL}\}^{(n)} \tag{8}$$

Suppose, as an example, the case of 1 DOF system and, for simplicity, assume that for this example only the first harmonic component is considered for the calculation.

Equation (6) can be rewritten as follows,

$$D^{(1)}\overline{X}^{(1)} - \overline{F}_{Ext}{}^{(1)} + \overline{F}_{NL}{}^{(1)} = R \tag{9}$$

Equation (9) cannot be solved directly because the first Fourier coefficient of the contact forces depends on the first Fourier coefficient of the displacement, so a nonlinear solver is required. The nonlinear solver starts from an initial guess, then a Newton iteration scheme minimizes the residual function. The main problem is that for each iteration the nonlinear force must be computed, and since it depends on the displacement, a mathematical law that binds these two quantities is needed. For this purpose, it is important to have a contact model that takes as input the displacement and comes out with the nonlinear Fourier coefficient. In this paper the 2D contact model is used, as shown in Figure 1.

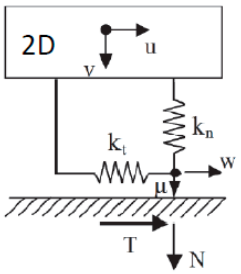

Figure 1. Contact model with variable normal load.

The contact model works in time domain and the non-linear forces in normal and tangential directions are defined by the following expressions,

$$N(t) = \max(k_n v(t), 0) \tag{10}$$

The computation of the tangential force is based on a predictor–corrector algorithm. This algorithm is explained in detail in [12]. The main outcomes are summarized below. The tangential force is computed by the algorithm at each time instant, under the assumption that the contact is in a stick state (predictor step).

$$T^P(t) = k_t(u(t) - w(t)) \tag{11}$$

The next step is the corrector one, in which the force computed in Equation (11) is compared with the Coulomb limit. Then, its value is recalculated as follows:

$$T(t) = \begin{cases} T^P(t) \ \text{ if } \left|T^P(t)\right| \le \mu N(t) \\ \mu N(t) \text{sign}\left(T^P(t)\right) \ \text{ if } \left|T^P(t)\right| \ge \mu N(t) \\ 0 \qquad\qquad \text{if } N(t) = 0 \end{cases} \tag{12}$$

The terms of previous equations are defined below:

- k_n is the normal stiffness
- $v(t)$ is the mass normal displacement
- k_t is the tangential stiffness
- $u(t)$ is the mass tangential displacement

- $w(t)$ is the contact element displacement
- μ is the friction coefficient between the mass and the ground
- $N(t)$ is the normal force
- $T^P(t)$ is the predicted tangential force
- $T(t)$ is the corrected tangential force

Equation (8) is written in frequency domain, but the output of the contact model is a nonlinear force in time domain, so a further step is necessary to obtain the first Fourier coefficient of the tangential nonlinear force. There are two possibilities for calculating $\bar{F}_{NL}^{(1)}$:

- The analytical expressions of the nonlinear force in time domain are written for all parts of the hysteresis cycle, and then its real and imaginary part can be obtained with Fourier integrals:

$$\Re\left(\bar{F}_{NL}^{(1)}\right) = \frac{1}{\pi}\int_0^{2\pi} F_{NL}(t)\cos(\omega t)dt \tag{13}$$

$$\Re\left(\bar{F}_{NL}^{(1)}\right) = \frac{1}{\pi}\int_0^{2\pi} F_{NL}(t)\cos(\omega t)dt \tag{14}$$

- The nonlinear force in time domain is switched in frequency domain using the FFT algorithm and, for this example, only the first harmonic component is considered.

The first approach is fully analytical and provides the theoretical value of the Fourier coefficients of the nonlinear force. However, it has a crucial drawback: it can only be applied when the hysteresis cycle is known a priori.

In practice, the hysteresis cycle is known in advance only in a few specific cases. Therefore, in real turbine applications, deriving analytical expressions for the nonlinear force is very difficult, if not impossible.

For this reason, the second approach is generally preferred and is also the most commonly used in the literature. The HBM combined with the time–frequency transformation is known as the AFT-HBM scheme, which was introduced by [22].

2.1. AFT-HBM

The AFT-HBM scheme is the harmonic balance method in which the Fourier coefficients are computed numerically with an FFT algorithm, which discretizes the Fourier integrals. Figure 2 shows the AFT-HBM calculation scheme applied to a 1 DOF system:

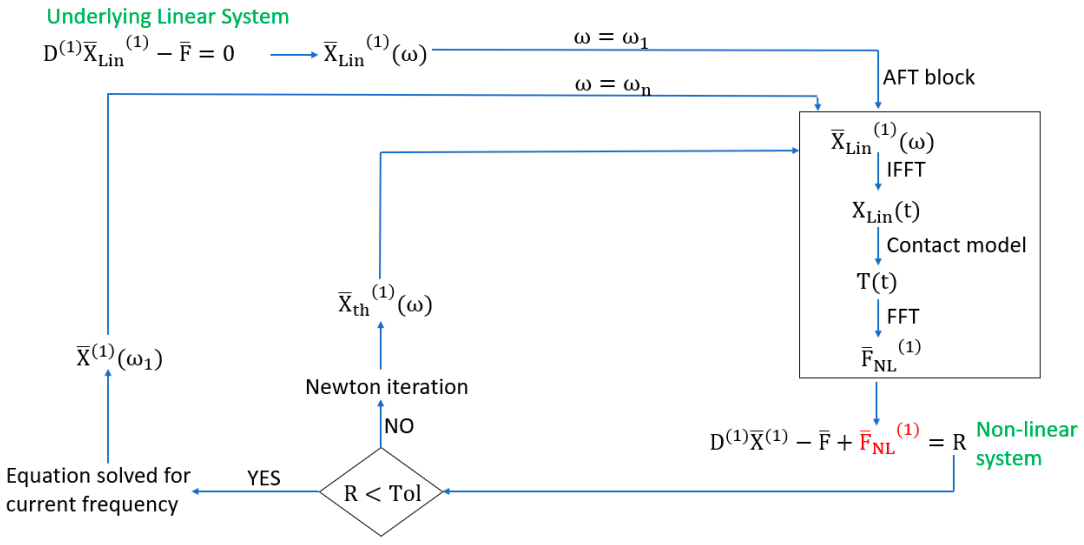

Figure 2. AFT-HBM calculation scheme.

For simplicity of notation in the calculation scheme represented in Figure 2, only the first harmonic component of the displacement and the nonlinear force is considered, but in real calculations, more harmonic components can be considered.

The AFT-HBM shown in the previous figure can be summarized in the following steps:

- The first step involves calculating the dynamic response of the underlying linear system in the frequency domain. This step is crucial as it provides an initial guess for the nonlinear solver, at least for the first frequency in the range of interest.
- The displacement computed for the first frequency of the range is the input for the AFT block, in which some further steps lead to the nonlinear force first Fourier coefficient computation.
- The input of the AFT block is a complex displacement, which through the IFFT algorithm is switched in time domain.
- The time domain displacement is used as input for the contact model, which comes out with the nonlinear force in time domain.
- The nonlinear force in time domain must be switched in frequency domain to be used in Equation (8). For this purpose, the FFT algorithm is used.
- The AFT block outputs the first Fourier coefficient of the nonlinear force, enabling the evaluation of the residual function at the initial frequency and iteration.
- If the value of the residual function is over the set tolerance, the solver did not reach the convergence; in this case a new Newton iteration is performed.
- If the value of the residual function is below the set tolerance, the convergence is reached and the solution at the first frequency is used as initial guess for solving the equation at the second frequency.
- This procedure is repeated until the convergence is achieved for each frequency of the frequency range of interest.

2.2. Pseudo Arc Length Continuation

The calculation scheme in Figure 2 works very well if during vibrations no detachment of contact surfaces occurs. This is a very simplified situation; in fact, in a real turbine application, when the blades are vibrating, there is a relative displacement between two adjacent sectors, which implies a relative displacement between the contact surfaces not only in the direction tangential to the contact but also in the direction normal to the contact itself. Normal relative displacement can significantly influence the non-linear response of the blades; in fact, during vibrations some points on contact surfaces can lose contact and regain contact intermittently. Intermittent contact has a direct influence on the FRF curve shape and so called "turning points" can appear. An example of a turning point is shown in Figure 3, where, for a single frequency, two or more solutions in terms of physical displacement are possible.

This behavior entails a problem during non-linear forced response calculation because near the turning point the Jacobian matrix of the system will become singular and the Newton iteration will fail.

When a turning point occurs the response curve is bent; this phenomenon cannot be captured with the natural continuation technique, which is essentially what is described in Figure 2. This scheme fails because with the classical continuation method the frequency step is set a priori for all the frequency range. As shown in the example in Figure 3, after the turning point, the curve goes towards lower frequencies, so if the next step is set as increasing frequency, the solver is trying to solve the equation in a point out of the solution curve, which leads to a lack of convergence.

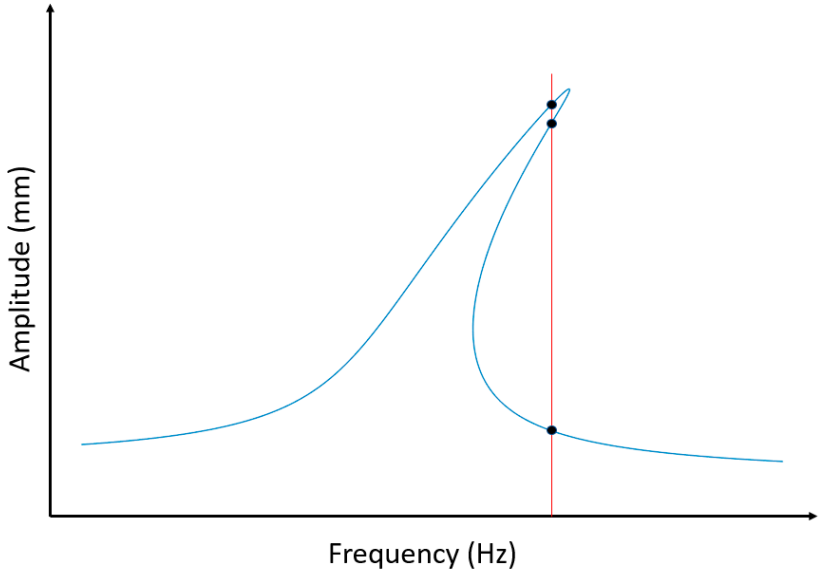

Figure 3. Turning point.

To avoid this issue, the frequency must not be imposed but should become an unknown of the problem; this concept is the idea behind the "Pseudo arc length continuation technique", widely described and applied to general bifurcation and non-linear eigenvalue problems by [23].

Now let us look at this technique from a graphical point of view in Figure 4:

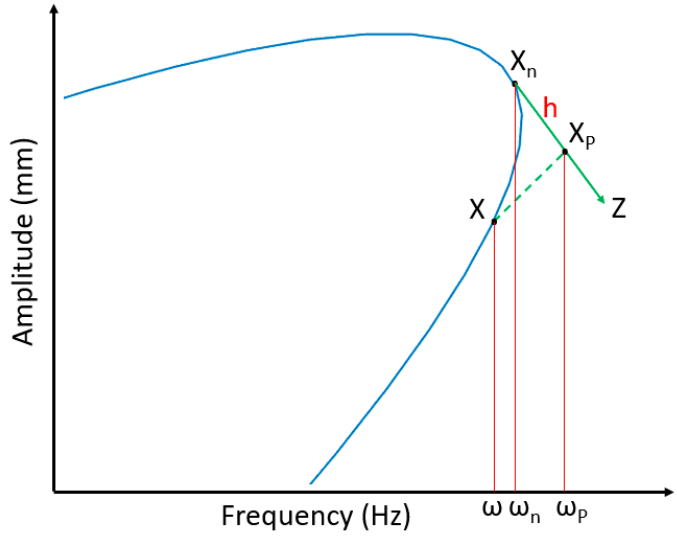

Figure 4. Graphical point of view of pseudo arc length continuation.

Before explaining in detail how "Pseudo arc length continuation" works, it is important to give some definitions for equations of motion:

- Z is the tangent vector calculated in the point X_n; it is defined with three components: $\begin{pmatrix} Z_1 \\ Z_2 \\ Z_3 \end{pmatrix}$.
- h is the step taken along the tangent vector to reach the predicted point.
- X_P, ω_P are the predicted point and the predicted frequency, respectively.
- X, ω are the searched point and the searched frequency, respectively.

- With X_P and ω_P a vector that will be used in equations of motion can be assembled; we will call it y_P and it is defined as follows: $\begin{pmatrix} \Re(X_P) \\ \Im(X_P) \\ \omega_P \end{pmatrix}$.
- The same reasoning can be employed with X and ω; we will call it y: $\begin{pmatrix} \Re(X) \\ \Im(X) \\ \omega \end{pmatrix}$.

Starting from point X_n, the goal is to find the point on the solution curve, X. The first step is to make a step h along the tangent vector Z (calculated in X_n) to reach the predicted point X_P.

From the predicted point some correction steps start until convergence is achieved. The main difference with respect to the classic continuation scheme is that the initial guess for the non-linear solver is not point X_n, but X_p. Starting from X_p some Newton iterations (correction steps) in parallel with "Pseudo arc length" constraint are needed to reach the solution point X.

The same procedure can be repeated starting from point X and so on until all the FRF curve is drawn.

Now this technique will be explained in detail from a mathematical point of view.

To embrace the pseudo arc length continuation in the AFT scheme, the residual function must be coupled with a linear constraint, so that the solution point lies on a line perpendicular to tangent vector. This constraint guarantees that starting from the predicted point the solution curve can be reached and the convergence achieved.

The augmented residual function, Equation (8), with pseudo arc length continuation constraint can be written as follows:

$$\begin{pmatrix} D^{(1)}\overline{X}^{(1)} - \overline{F}_{Ext} + \overline{F}_{NL}{}^{(1)} = R_1 \\ \left(y_p - y\right)^T Z = R_2 \end{pmatrix} \tag{15}$$

$$\begin{pmatrix} \begin{bmatrix} D_{11} & D_{12} \\ D_{21} & D_{22} \end{bmatrix}^{(1)} \begin{pmatrix} \Re\left(\overline{X}^{(1)}\right) \\ \Im\left(\overline{X}^{(1)}\right) \end{pmatrix} - \begin{pmatrix} \Re\left(\overline{F}_{Ext}\right) \\ \Im\left(\overline{F}_{Ext}\right) \end{pmatrix} + \begin{pmatrix} \Re\left(\overline{F}_{NL}{}^{(1)}\right) \\ \Im\left(\overline{F}_{NL}{}^{(1)}\right) \end{pmatrix} = \begin{pmatrix} \Re(R_1) \\ \Im(R_1) \end{pmatrix} \\ \left(\begin{pmatrix} \Re\left(\overline{X}_P{}^{(1)}\right) \\ \Im\left(\overline{X}_P{}^{(1)}\right) \\ \omega_P \end{pmatrix} - \begin{pmatrix} \Re\left(\overline{X}^{(1)}\right) \\ \Im\left(\overline{X}^{(1)}\right) \\ \omega \end{pmatrix} \right)^T \begin{pmatrix} Z_1 \\ Z_2 \\ Z_3 \end{pmatrix} = R_2 \end{pmatrix} \tag{16}$$

To clarify Figure 4, the physical displacements correspond to the norm of the complex displacement, whereas the equations of motion use the real and imaginary parts of the displacement.

The first term of the residual function in Equation (14) is the same as the previous equation but is expressed with real and imaginary parts of the complex terms. The second term is the pseudo arc length continuation constraint. Mathematically, it is the scalar product between the vector from the predicted point to the desired one and the tangent vector. The minimization of the second term of the residual function means that the previously mentioned vectors are perpendicular. This guarantees a prescribed direction for the correction steps and the convergence of the solver.

It can be noticed that the augmented residual function now has three components, so the frequency becomes an unknown in the problem, which allows us to get around turning points, making it possible to avoid convergence issues.

Figure 5 shows the AFT scheme with pseudo arc length continuation constraint:

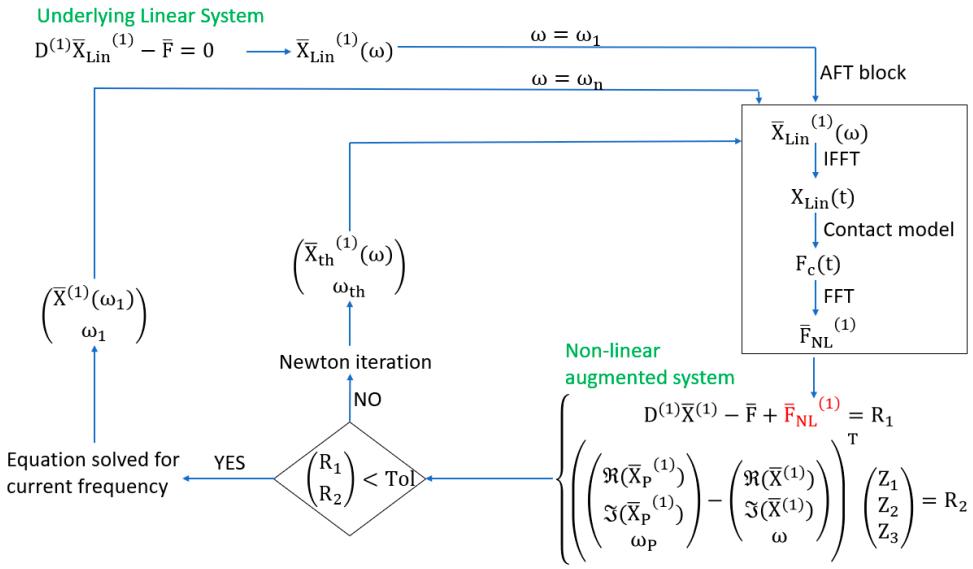

Figure 5. AFT-HBM calculation scheme with pseudo arc length continuation constraint.

The calculation scheme in Figure 5 is very similar to the one shown in Figure 2. The main difference is the residual function, which in this case includes the pseudo arc length continuation constraint.

The non-linear solver must minimize simultaneously the two residual terms. With this implementation the frequency is no longer fixed a priori but comes out as a solution of the equations system. This calculation scheme makes it possible to get around turning points and avoid convergence issues.

3. Test Case: 1 DOF System with Variable Normal Load

The chosen test case presented in this paper is a 1 DOF system connected to an inclined surface with the contact element of Figure 1, which can also capture the normal load variation, whose effect is widely discussed by [24]. There are two possible different configurations of the test case:

- The contact element is initially separated from the ground, so there is a negative gap, which is defined as $-\frac{N_0}{K_n}$.
- The contact element is initially in contact with a positive preload acting on the contact element; in this case a positive gap can be defined as $+\frac{N_0}{K_n}$.

The test case is shown in Figure 6:
All system parameters are defined below:

- K is the spring stiffness.
- C is the system damping.
- M is the mass of the system.
- X is the physical displacement
- F_0 is the external excitation amplitude.
- k_t is the contact tangential stiffness.
- k_n is the contact normal stiffness.
- N_0 is the normal preload acting on the contact element.
- u is the mass tangential displacement in the contact reference system.
- v is the mass normal displacement in the contact reference system.
- gap is the initial gap between the mass and the ground.

- w is the tangential displacement of the contact element.

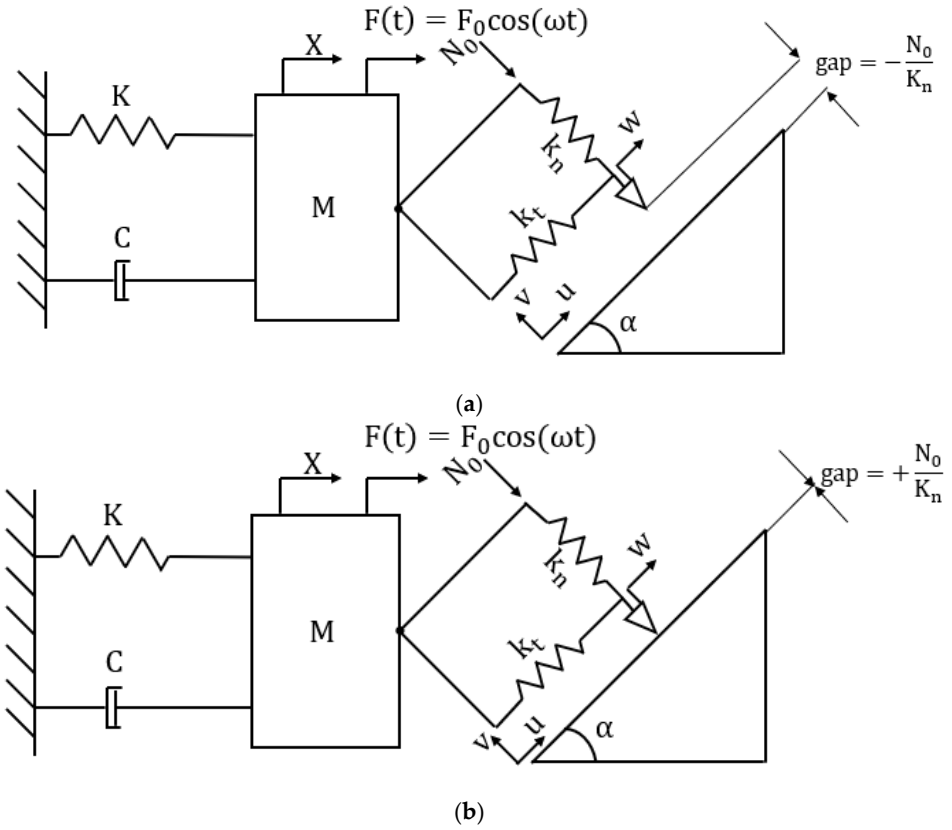

Figure 6. (**a**) Test case with negative gap configuration; (**b**) test case with positive gap configuration.

For all calculations performed in this section, only one harmonic component is considered.

The contact parameters adopted in this section and in the next one are chosen considering the typical order of magnitude of stiffness values used in the literature for 1 GDL systems [25]. These values are not linked to physical properties of a real contact surface because the focus here is a sensitivity analysis that is independent from the method used for the stiffness values choice.

The first calculation, case A, is carried out with a positive gap value, the computation parameters are reported in Table 1:

Table 1. Computation parameters for case A.

Parameter	Units	Value
M	Kg	1
K	$\frac{N}{mm}$	40
C	$\frac{Ns}{mm}$	0.4
K_t	$\frac{N}{mm}$	100
K_n	$\frac{N}{mm}$	200
M	/	0.3
A	rad	$\frac{\pi}{4}$
Gap	mm	0.5

The external excitation is varied from 1 to 10 N; the non-linear FRF curves obtained are shown in Figure 7:

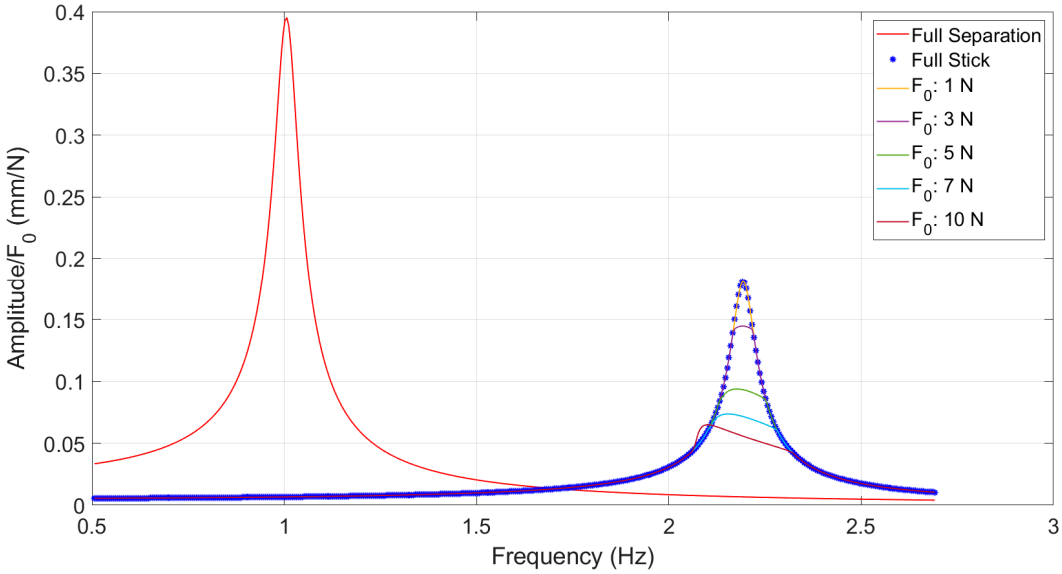

Figure 7. Non-linear response with fixed positive gap and different excitation levels.

The non-linear curves in Figure 7 are obtained by fixing the gap value and varying the excitation level amplitude. For this example, a gap value of 0.5 mm is set. The gap value determines the normal static preload on the contact element because it is defined as $\mp\frac{N_0}{k_n}$; in this case the static preload is 50 N.

The first non-linear curve, the yellow one, is overlapped to the stick linear response; this is happening because the excitation level is not enough to reach the slip condition and the mass is spending all the vibration period stuck to the ground, so there is no friction and the system behaves as a linear system.

Increasing the excitation level, the vibration amplitude is larger, which leads to frictional forces between the mass and the ground, and some kinetic energy is dissipated. In fact the maximum amplitude of the non-linear curves shows an inverse trend with the excitation level.

An important observation that can be drawn from Figure 7 is about the non-linear FRF curves shape. With the calculation parameters used for this example, the normal load is, of course, varying because the ground is inclined with respect to the mass, so on the contact coordinate system, there is also a variable normal component of the displacement but no turning points appeared. This is happening because the net normal load is the sum of the static preload and the dynamic one for every time instant. In this case the excitation levels used are not enough to cause the detachment between the mass and the ground, so no intermittent contact occurs. This makes the use of pseudo arc length continuation unnecessary, as the calculation scheme shown in Figure 2 is sufficient.

This case is a simplified situation. In fact in real applications the detachment of contact surfaces can occur, and the solver must be able to capture turning points due to the intermittent contact.

The next calculation, case B, will be performed with the same gap value, but this time it will be set as negative. The same values are assumed for the excitation level.

Calculation parameters are shown in Table 2:

Table 2. Computation parameters for case B.

Parameter	Units	Value
M	Kg	1
K	$\frac{N}{mm}$	40
C	$\frac{Ns}{mm}$	0.4
k_t	$\frac{N}{mm}$	100
k_n	$\frac{N}{mm}$	200
M	/	0.3
A	rad	$\frac{\pi}{4}$
Gap	mm	-0.5

Figure 8 shows both the results obtained with the negative and the positive gap values.

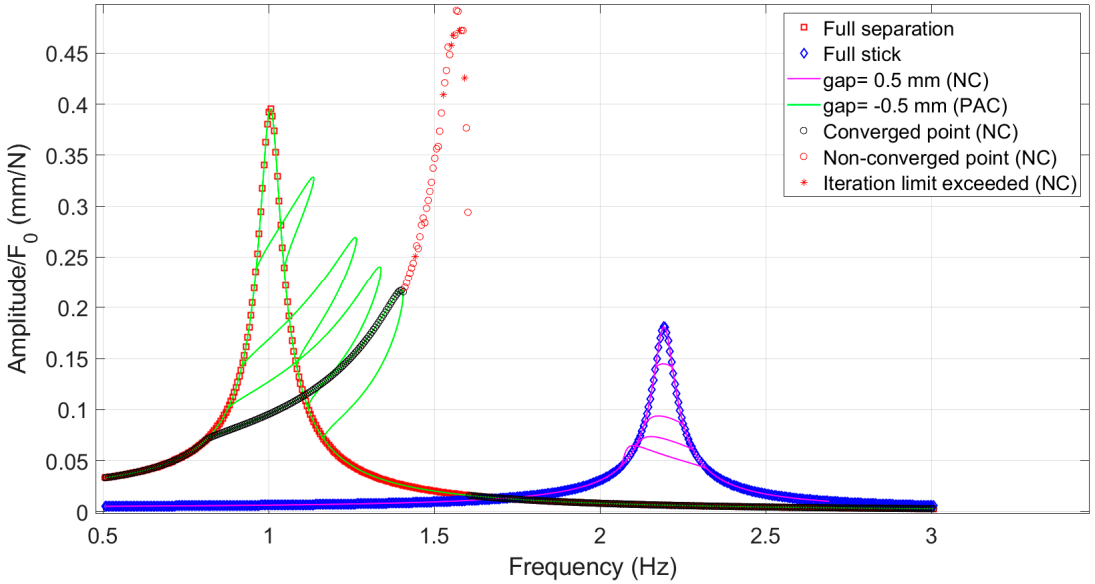

Figure 8. Non-linear response with fixed gap value (positive and negative) and varying excitation levels.

By observing Figure 8, some considerations can be made. First, the gap value has a significant influence on the non-linear FRF shape and thus on the calculation scheme that must be adopted. For this case using the same excitation levels, changing only the gap sign, the non-linear response shows turning points because intermittent contact occurs, so the calculation scheme in Figure 5 has to be adopted.

The FRF obtained with 1 N of excitation level and -0.5 mm gap is overlapped with the full-separation linear FRF. This happens because the excitation is not enough to bring the mass into contact with the ground.

Fixing the excitation level to 10 N and the gap value to -0.5 mm, a calculation without pseudo arc length continuation scheme is performed. What can be observed in Figure 8 is that the calculation fails near the turning point; in fact, there are a lot of points that do not reach the convergence and the solution jumps to the right solution branch only beyond a certain frequency value. This happens because the natural continuation is not able to get around turning points and trace the unstable solution branch.

Another important point is the calculation time, which of course is affected by the adopted calculation scheme. When the pseudo arc length continuation scheme is adopted, the frequency comes out as a solution of the augmented system and the frequency step is lower with respect to the natural continuation, and thus the calculation time is higher. The calculation time for the FRF obtained with 10 N of excitation and 0.5 mm of gap is

5.2 s, while the time for calculating the same FRF with the pseudo arc length continuation technique is 38.6 s. There is a non-negligible difference between the two computation times, so it is important to use the pseudo arc length continuation technique only when it is necessary to not unnecessarily increase the non-linear solver computation effort.

The above calculations show how the combination of gap and excitation level significantly influence the non-linear response. A further calculation, fixing the excitation level to 100 N and varying the gap from −5 mm to 3 mm, is performed. Calculation parameters are reported in Table 3:

Table 3. Computation parameters.

Parameter	Units	Value
M	Kg	1
K	$\frac{N}{mm}$	40
C	$\frac{Ns}{mm}$	0.4
k_t	$\frac{N}{mm}$	100
k_n	$\frac{N}{mm}$	10^3
μ	-	0.3
α	rad	$\frac{\pi}{4}$

Obtained FRF curves are shown in Figure 9:

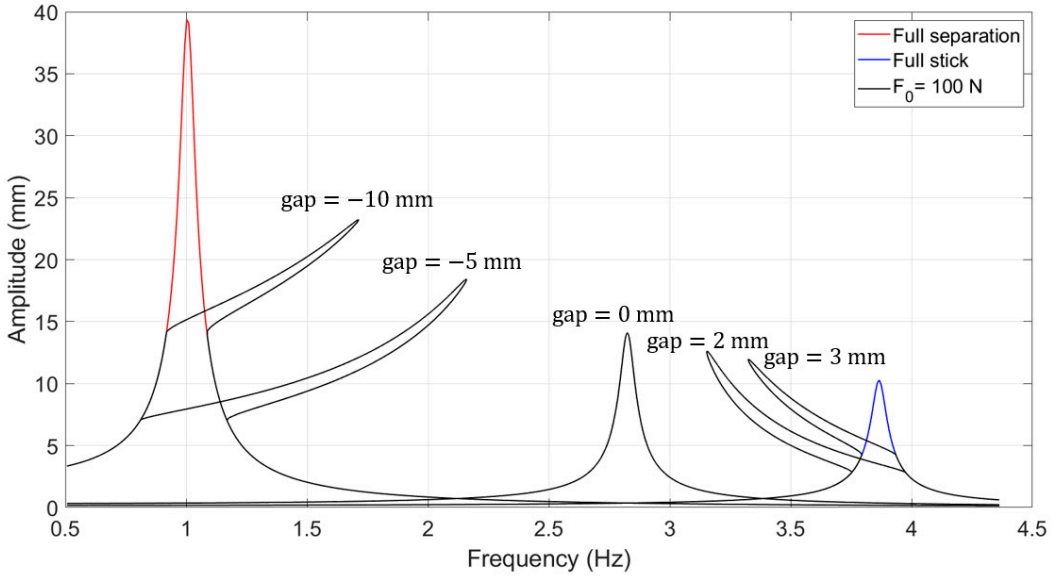

Figure 9. Non-linear response with fixed excitation level and different gap values.

In Figure 9 different gap values for a fixed excitation are explored. It can be observed that with positive gap values (positive normal pre-load on the contact element), if the excitation level is large enough, intermittent contact occurs, and the pseudo arc length continuation technique is necessary to ensure the solver convergence.

4. Sensitivity Analysis: Time Samples per Period, Harmonic Truncation Order and Contact Parameters

This section will be focused on a sensitivity analysis on the main parameters that can affect the non-linear solver convergence. The first-discussed parameter is the number of time samples per period. The harmonic order truncation will then be discussed, and finally the effect of contact parameters. For this sensitivity analysis two specific cases are considered:

- Case 1: 10 N of excitation level and 0.5 mm of gap. The other calculation parameters are the same reported in Table 1.
- Case 2: 100 N of excitation level and −5 mm of gap. The other calculation parameters are the same as those reported in Table 3.

4.1. Time Samples per Period

Time samples per period is a very crucial parameter because it determines the number of points in which the displacement and the non-linear force are discretized in time domain. Figure 10 shows in more detail the AFT procedure that was mentioned in Figures 2 and 5:

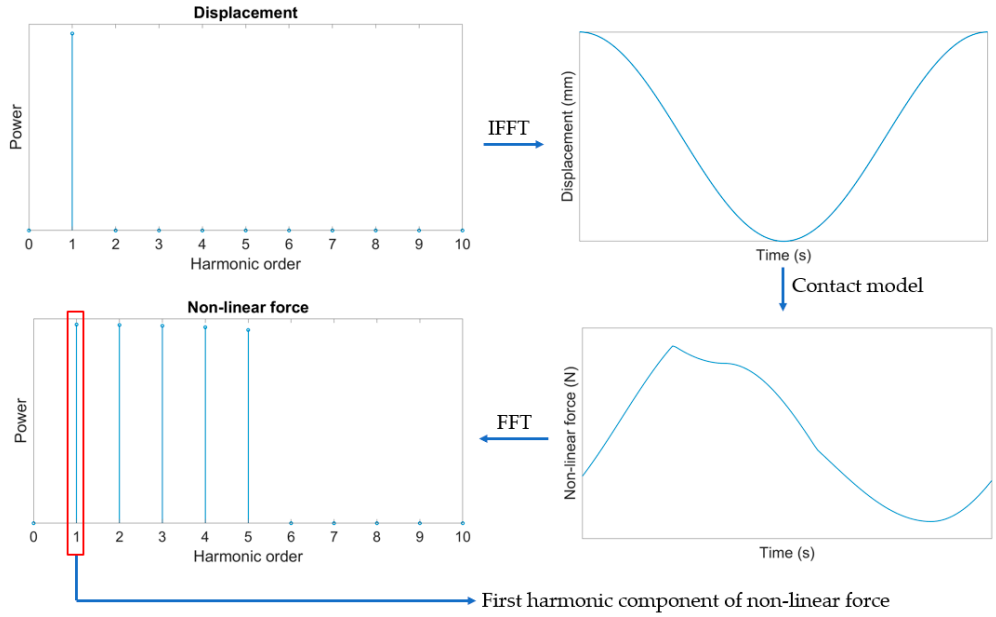

Figure 10. AFT scheme representation.

The AFT scheme can be summarized in the following steps:

- The complex displacement in frequency domain is processed by IFFT algorithm and becomes a time domain signal.
- The displacement time signal is the input for the contact model, in which the non-linear force in time domain is computed.
- The signal of the non-linear force in time domain is processed with the FFT algorithm and the Fourier coefficients of the non-linear force are computed.

Note: the scheme in Figure 10 refers to a situation in which only the first harmonic component is taken; in general, the harmonic truncation order can be higher than 1, but this will be discussed in the next subsection.

From the AFT scheme, the importance of the number of time samples per period can be understood. In fact, if this parameter is not large enough, the time signal of the non-linear force is badly discretized, and the Fourier coefficient is not correctly computed.

Let us consider case 1: the number of time samples per period is varied from 5 to 2^7, and the obtained results are shown in Figure 11:

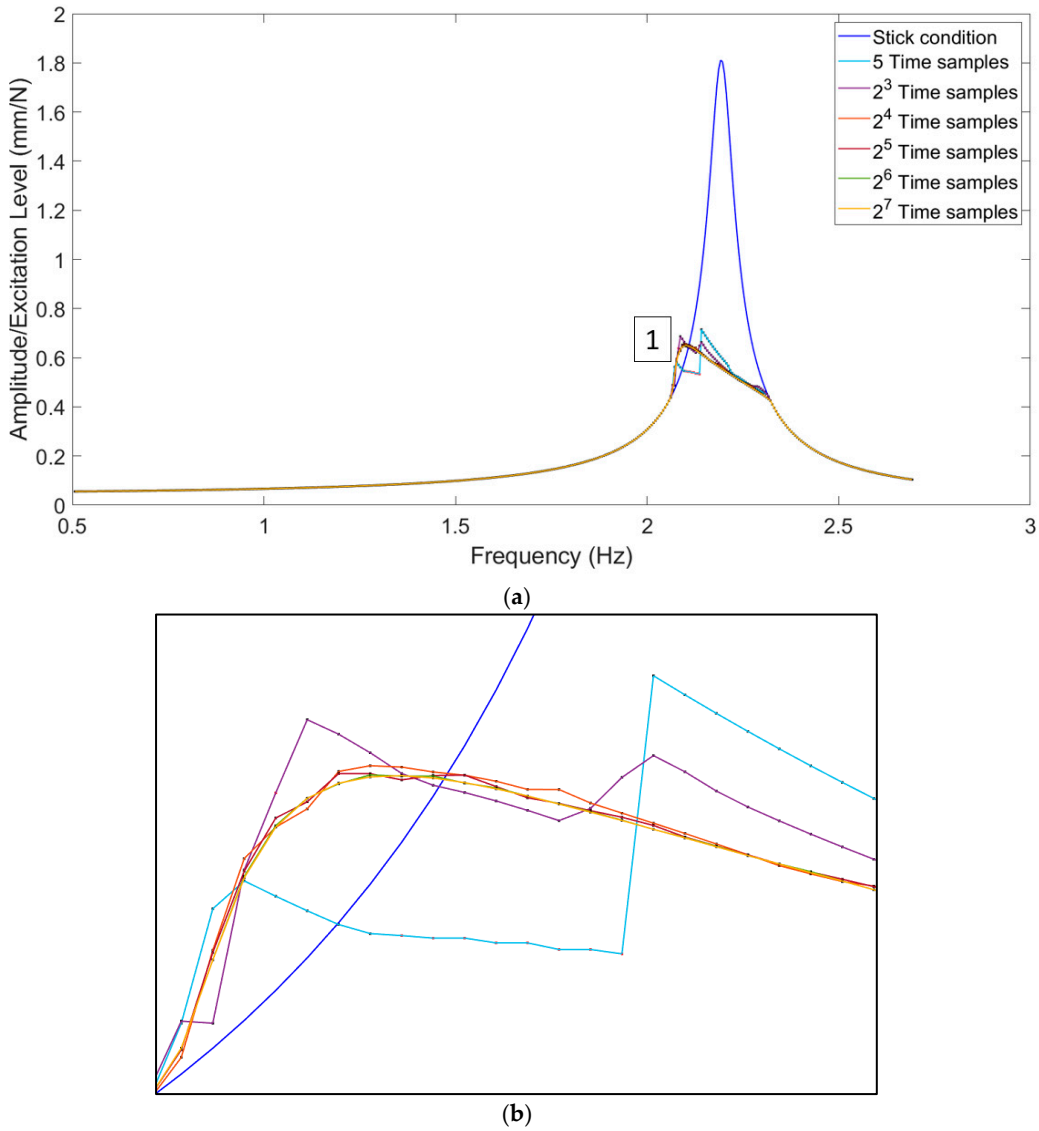

Figure 11. (**a**) Non-linear response for case 1 varying the number of time samples per period. (**b**) Zoom on 1.

The FRF curves shown in Figure 11 are obtained considering only one harmonic component, so the minimum number of time samples, according to [21], is five and can be written as $4H + 1$, in which H is the harmonic order truncation. Using just five samples per period, certain points on the curve do not reach convergence, making the FRF shape appear irregular. This happens because using fewer numbers of time samples leads to aliasing errors.

Aliasing depends on the non-linear force signal in time domain, which alternates between time instants when the system is in stick condition and time instants when it is in slip one (non-smooth signal), so if there are not enough points to capture stick–slip transitions when FFT is applied to the signal, the resulting Fourier coefficients are not properly calculated.

This phenomenon is known as the Gibbs phenomenon and occurs when trying to approximate with Fourier series a function that has jump discontinuities. Around the discontinuities, even when increasing the number of harmonics, oscillations persist, which does not allow the signal to be optimally approximated. Everything about the Gibbs phenomenon from a mathematical point of view is widely discussed by [26].

When increasing the time samples, aliasing errors decrease and the FRF shape becomes smoother. For this case, 2^4 points are enough to avoid aliasing errors, but 2^7 points are necessary to not have irregularities.

Let us now consider case 2: the number of samples per period is varied from 2^6 to 2^{12}, and the results are reported in Figure 12:

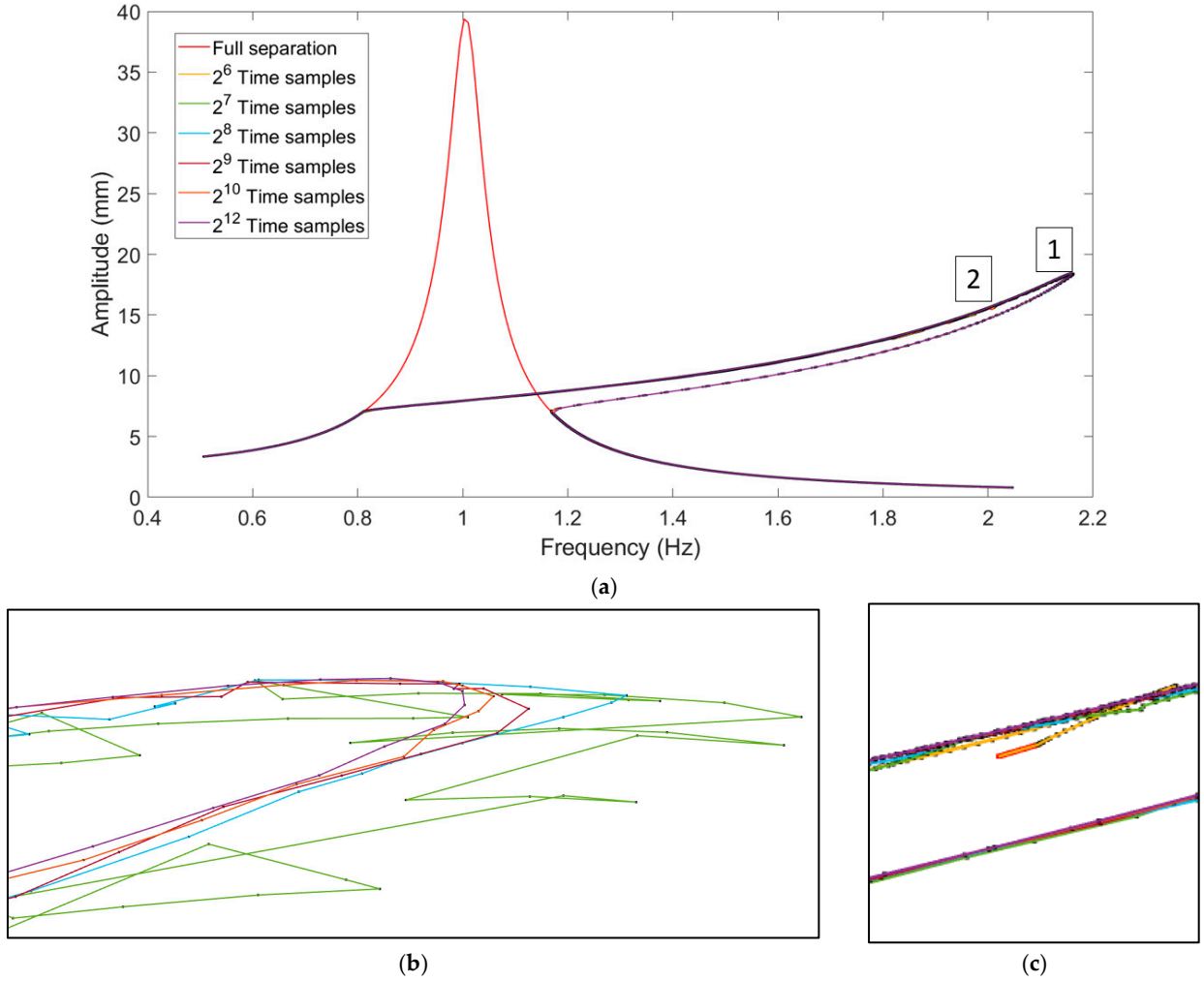

Figure 12. (**a**) Non-linear response for case 2 varying the number of time samples per period. (**b**) Zoom on 1. (**c**) Zoom on 2.

In the FRF curves in Figure 12, in which intermittent contact occurs, the effect of time samples is more evident and more critical. This happens because intermittent contact generates an infinite sequence of decaying, but non-zero, Fourier coefficients for a harmonic input, as well explained and described by [14]. For this reason, aliasing errors due to truncation of Fourier series cannot be avoided with an AFT scheme and this leads to the necessity to oversample the time signal to reduce numerical oscillations and to ensure the solver convergence.

The first difference that can be noticed between curves in Figures 11 and 12 is the number of time samples per period needed for avoiding non-converged solutions. In fact for the first case, 2^6 time samples are enough to not have aliasing errors and to avoid oscillations in FRF, while in the second one with the same time samples, the solver is not able to converge and the calculation fails.

The minimum number of time samples to reach convergence in the second case is 2^7, but as can be seen in Figure 12, numerical oscillations occur due to the Fourier series

truncation. When increasing the number of time samples, numerical oscillations decrease and beyond a certain value are minimized. In this case, 2^{10} time samples were required to drastically reduce numerical oscillations.

Unfortunately, to the authors' knowledge, this parameter does not reach a plateau. In fact there is no value above which aliasing issues can be completely avoided but must be set according to the specific case. With awareness of this, when systems exhibit intermittent contact, it is better to oversample, even for harmonic inputs.

The computation times for case 1 and case 2 are also calculated, and the results are reported in Tables 4 and 5:

Table 4. Computation times for case 1.

Time Samples	Computation Time	Units
2^4	2.85	S
2^5	2.92	S
2^6	3.12	S
2^7	3.49	S

Table 5. Computation times for case 2.

Time Samples	Computation Time	Units
2^7	35.2	s
2^8	64.4	s
2^9	69.9	s
2^{10}	54.04	s
2^{12}	71.57	s

What can be concluded from this first sensitivity analysis is that the number of time samples per period is a very crucial parameter for the non-linear solver convergence, especially when intermittent contact occurs.

The solver's lack of convergence when there is no intermittent contact can be avoided using a number of samples slightly above the minimum value; on the other hand, if there is intermittent contact, aliasing errors cannot be avoided, but the solver convergence may be improved by oversampling the non-linear force time signal.

Oversampling improves the solver convergence but of course affects computation times. In fact, observing previous tables, the increase in computation time is strictly correlated to an increase in the number of time samples per period. The only exception is with 2^{10} time samples; this can be explained by the fact that when passing from 2^9 to 2^{10} time samples, numerical oscillations are drastically reduced, and the number of iterations needed for reaching convergence decreases.

In conclusion, it is important to use the right number of time samples per period to avoid convergence issues, but unnecessary oversampling increases computational effort without further improvement of a non-linear calculation response.

4.2. Harmonic Truncation Order

In this subsection the effect of the harmonic truncation order will be discussed, in particular two subcases of case 1 an two subcases of case 2 will be considered:

- Subcase 1: excitation level: 10 N, gap: 0.5 mm, 2^4 time samples per period, harmonic truncation order: $1-3$
- Subcase 2: excitation level: 10 N, gap: 0.5 mm, 2^7 time samples per period, harmonic truncation order: $1, 5, 7, 10$

- Subcase 3: excitation level: 100 N, gap: -5 mm, 2^8 time samples per period, harmonic truncation order: $1, 5, 7, 10$
- Subcase 4: excitation level: 100 N, gap: -5 mm, 2^{10} time samples per period, harmonic truncation order: $1, 5, 7, 10$

The results obtained for subcase 1 are shown in Figure 13:

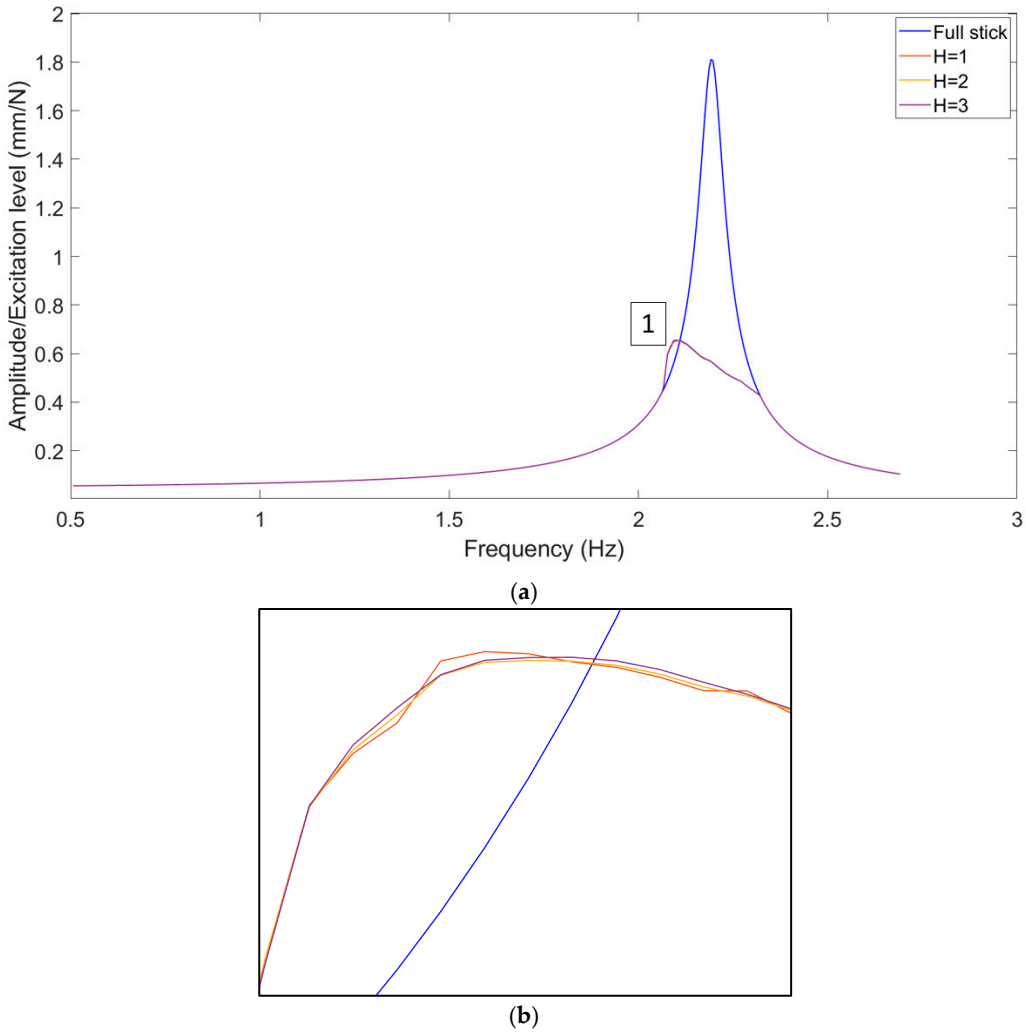

Figure 13. (**a**) Subcase 1 non-linear response for different harmonic truncation orders. (**b**) Zoom on 1.

When increasing the number of harmonic components considered in the calculations, the non-linear FRF changes, albeit only slightly in this case, because the time signal of the non-linear force is better approximated, and the Fourier coefficients calculated with FFT are more accurate.

It is interesting to observe that there are still some irregularities on the FRF curves when using more harmonic components. This is due to aliasing errors, which mainly depend on the number of time samples per period.

Let us now consider subcase 2. The results are reported in Figure 14:

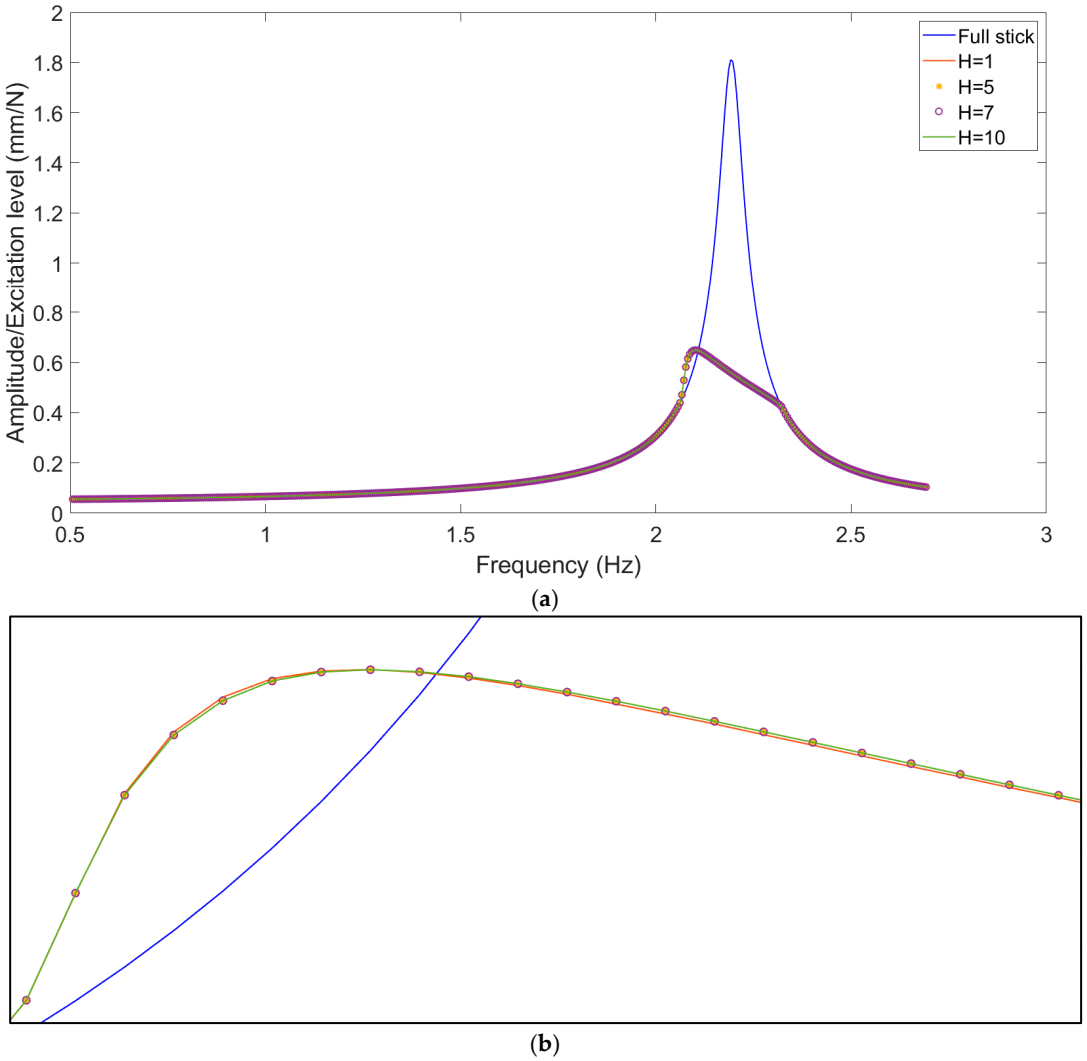

Figure 14. (**a**) Subcase 2 non-linear response for different harmonic truncation orders. (**b**) Zoom on 1.

In this case the harmonic truncation order was varied from 1 to 10 harmonic components. Observing Figure 14, it can be noticed that when increasing the harmonics the non-linear FRF varies less than in the previous case, and also with only one harmonic component the non-linear response is very similar to the one calculated with 10 harmonic components.

Summarizing these first two calculations, we can conclude the following:

- Using too few time samples per period leads to aliasing errors, which persist even when increasing the harmonic truncation order.
- Conversely, choosing enough time samples to avoid aliasing errors, even with just one harmonic component, can yield an accurate nonlinear response without irregularities.

When considering subcase 3 and subcase 4, for the next two calculations intermittent contact occurs, so we expect a different non-linear behavior. Results are shown in Figures 15 and 16:

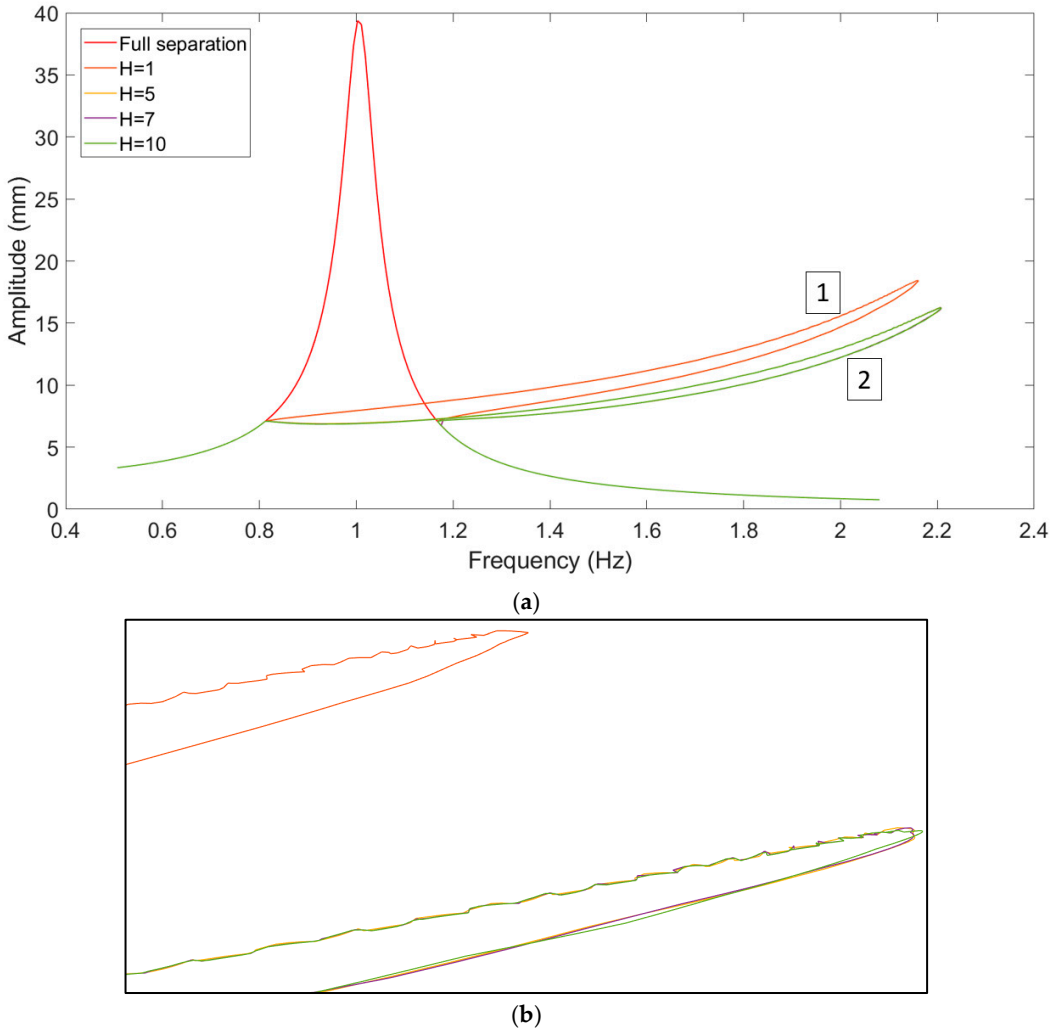

Figure 15. (**a**) Subcase 3 non-linear response for different harmonic truncation orders. (**b**) Zoom on 1 and 2.

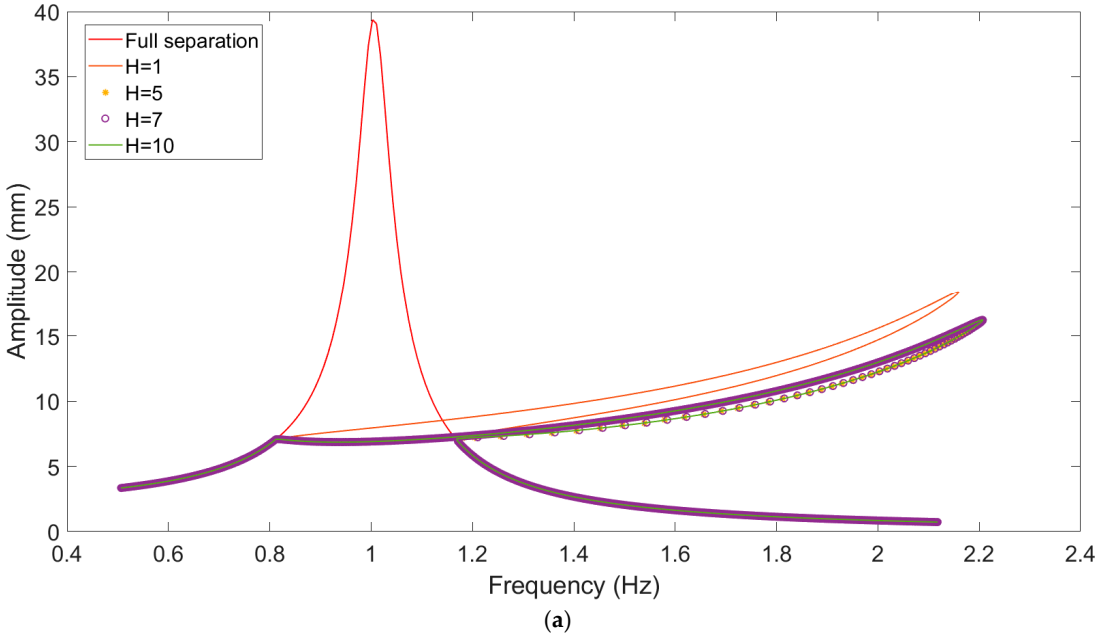

Figure 16. *Cont.*

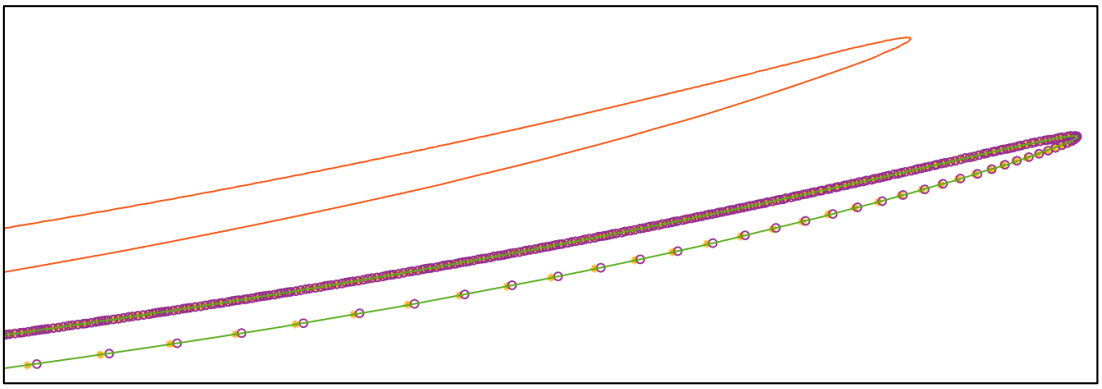

(**b**)

Figure 16. (**a**) Subcase 4 non-linear response for different harmonic truncation orders. (**b**) Zoom on 1 and 2.

When intermittent contact occurs the effect of harmonic truncation order and time samples per period is more evident. In fact by observing Figure 15 a big difference can be noticed between non-linear curves obtained with different truncation orders.

In this case five harmonics are enough to approximate the solution. In fact the FRF curves calculated with 5, 7 and 10 harmonics are overlapped.

Regarding the number of samples per period, numerical oscillations still persist, even when increasing the number of harmonics, due to the issues extensively discussed in the previous subsection.

In Figure 16 there is the same trend with harmonic order truncation of course, but numerical oscillations are drastically reduced by increasing the number of time samples per period.

What was discussed about harmonic truncation order can be summarized as follows:

- When increasing the number of harmonic components, the non-linear response is better approximated, especially when there is intermittent contact, which generates a force signal that requires higher harmonics to be approximated with Fourier series.
- Increasing the number of harmonic components but using a poor number of time samples still leads to numerical oscillations and sometime to convergence issues, also without intermittent contact.

It is also interesting to investigate computation times for all explored cases in this subsection. The results are reported in Tables 6–9:

Table 6. Computation times for subcase 1.

Harmonic Truncation Order	Computation Time	Units
1	2.97	s
2	3.92	s
3	4.87	s

Table 7. Computation times for subcase 2.

Harmonic Truncation Order	Computation Time	Units
1	3.32	s
5	8.92	s
7	12.49	s
10	18.77	s

Table 8. Computation times for subcase 3.

Harmonic Truncation Order	Computation Time	Units
1	64.4	s
5	83.94	s
7	192.43	s
10	183.14	s

Table 9. Computation times for subcase 4.

Harmonic Truncation Order	Computation Time	Units
1	54.04	s
5	166.44	s
7	228.14	s
10	420.4	s

The main outcome of this subsection is that there is a not-negligible difference between the cases in which there is no intermittent contact and the cases in which there is. In the first situation, beyond a certain value of time samples per period, aliasing errors are completely avoided and the non-linear response can be well calculated with harmonic truncation order 1; this leads to low computational effort.

For the second situation, a harmonic truncation order 1 is not enough to compute the correct non-linear FRF. In fact, in this case, a minimum harmonic order truncation of 5 is required. In addition to this, several time samples per period are needed to avoid numerical oscillations. In this case, 2^{10} are required.

In conclusion, the number of time samples per period is the most limiting factor in terms of solver convergence, but it must be coupled with a properly harmonic truncation order to avoid convergence issues and to compute the right FRF curve. This leads to high computational effort when intermittent contact occurs. For this reason, the signal oversampling and the harmonic order truncation must be set to proper values to not unnecessarily increase the solver computation time.

4.3. Contact Parameters

This subsection is focused on exploring the effect of contact parameters on the non-linear response. In particular, the case with intermittent contact is considered since it is more critical and more commendable. In detail, two cases are explored:

- Case 1: the k_t is set to $10^2 \frac{N}{mm}$, the k_n is varied from $2 * 10^2$ to $10^5 \frac{N}{mm}$, $F_0 = 100$ N, gap $= -5$ mm. The calculation is performed considering only one harmonic component.
- Case 2: the k_n is set to $10^3 \frac{N}{mm}$, the k_t is varied from $2 * 10^2$ to $10^4 \frac{N}{mm}$, $F_0 = 100$ N, gap $= -5$ mm. The calculation is performed considering only one harmonic component.

Let us consider the first case. The results are shown in Figure 17.

The effect of normal stiffness variation is clearly visible in Figure 17. By increasing its value, there is a major stiffening when intermittent contact occurs. This stiffening effect can be well appreciated from previous figures. In fact, as normal stiffness increases, the non-linear FRF bend more to high frequencies, and the maximum displacement near the resonance decreases and the curve becomes thinner.

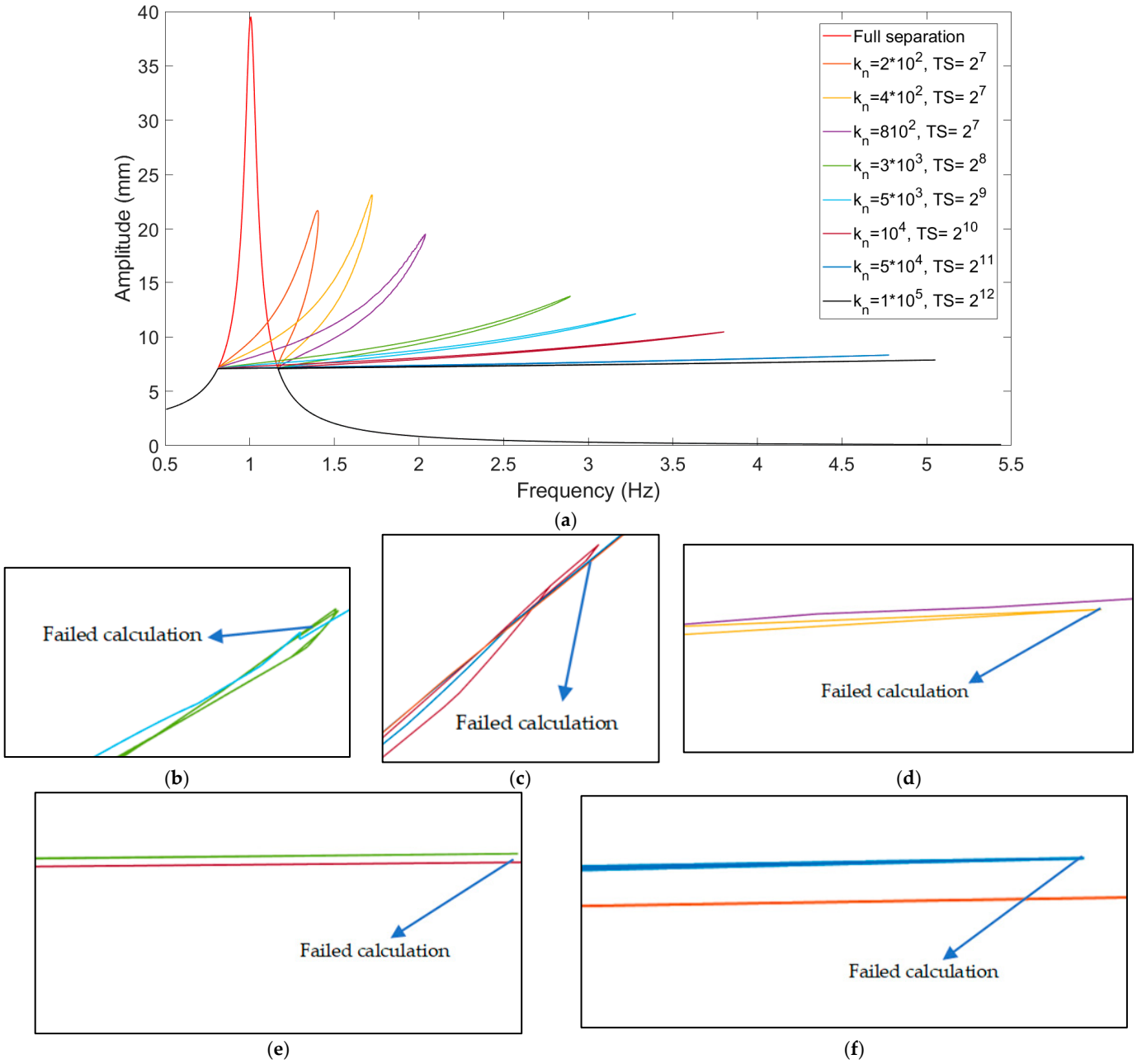

Figure 17. (**a**) Case 1 non-linear response. (**b**) Failed calculation with 2^7 time samples and $k_n = 3 * 10^3 \frac{N}{mm}$. (**c**) Failed calculation with 2^8 time samples and $k_n = 5 * 10^3 \frac{N}{mm}$. (**d**) Failed calculation with 2^9 time samples and $k_n = 10^4 \frac{N}{mm}$. (**e**) Failed calculation with 2^{10} time samples and $k_n = 5 * 10^4 \frac{N}{mm}$. (**f**) Failed calculation with 2^{11} time samples and $k_n = 10^5 \frac{N}{mm}$.

Observing the legend in Figure 17, it is interesting to see the trend of the time samples per period with the normal stiffness value. Increasing the normal stiffness induces more intermittent contact leading to greater high harmonics contributions. Aliasing errors may occur if the force time signal is not oversampled, even when only the first harmonic component is used in the calculation.

For typical stiffness values between 200 N/mm and 800 N/mm, 2^7 time samples per period are sufficient to ensure convergence. However, as the stiffness increases, a greater number of samples is required to prevent aliasing errors. In this example, with a stiffness of 10^4 N/mm, 2^{12} time samples were necessary to avoid convergence issues. This number

of samples is significantly higher than the theoretical requirement for calculating a single harmonic component.

Let us now consider case 2; the obtained results are shown in Figure 18:

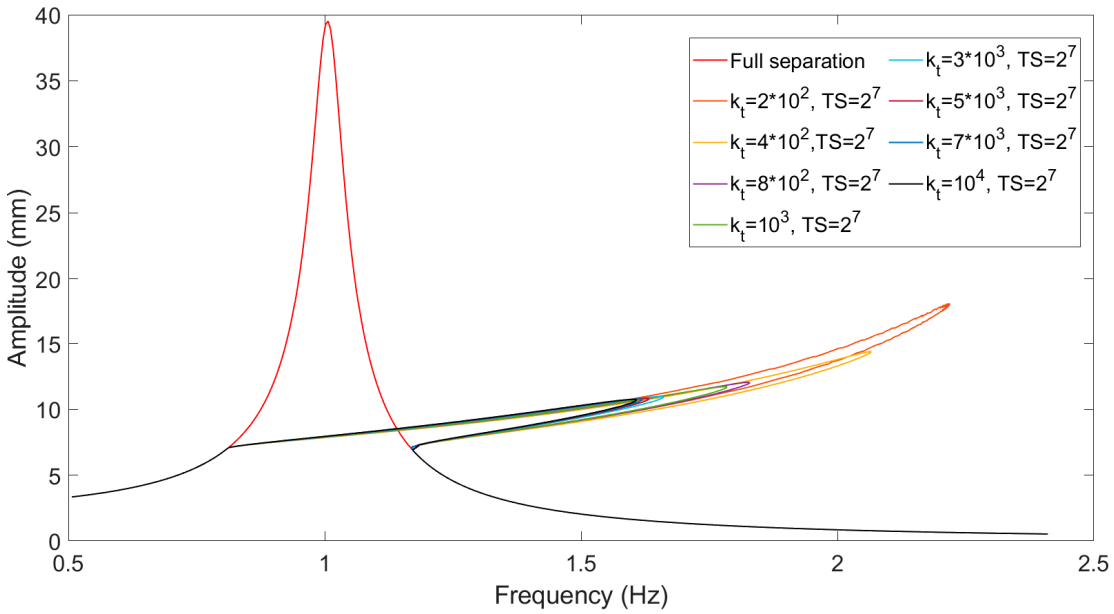

Figure 18. Non-linear response for case 2.

Case 2 exhibits a markedly different behavior compared with the first situation. As the tangential stiffness increases, the nonlinear Frequency Response Function (FRF) does not shift toward higher frequencies; instead, the resonance peak moves to lower frequencies. This phenomenon can be explained by the fact that higher tangential stiffness results in an increased frictional force between the mass and the ground. Consequently, displacements near resonance become smaller, leading to reduced detachment between the contact surfaces.

In this case, 2^7 time samples per period are sufficient to achieve convergence, although minor numerical oscillations may still be observed. As shown in Figure 18, 2^7 samples ensure solver convergence across all examined tangential stiffness values. This contrasts with the previous case, where up to 2^{12} time samples per period were necessary to achieve convergence at the highest normal stiffness value.

This difference can be attributed to the fact that higher tangential stiffness reduces the extent of intermittent contact. As a result, aliasing errors can be avoided even with a lower number of time samples used to discretize the nonlinear force in the time domain.

The main findings from this section can be summarized as follows:

- Normal stiffness has a greater impact than tangential stiffness on the required number of time samples per period.
- Beyond certain thresholds of normal stiffness, significant oversampling is necessary to ensure solver convergence.
- The number of time samples per period becomes the most critical factor in the computation when intermittent contact is present.

5. Computation with Real Blade Contact Parameters

The calculations presented in Section 4.3 were intended to illustrate how the nonlinear response varies with changes in contact parameters; therefore, the parameter values were chosen to highlight general trends. In this section, the focus shifts to calculations performed

using realistic contact parameters, with the aim of simulating the forced response of a blade under actual contact conditions.

Figure 19 shows a portion of a real steam turbine model with a snubber as a dry friction device:

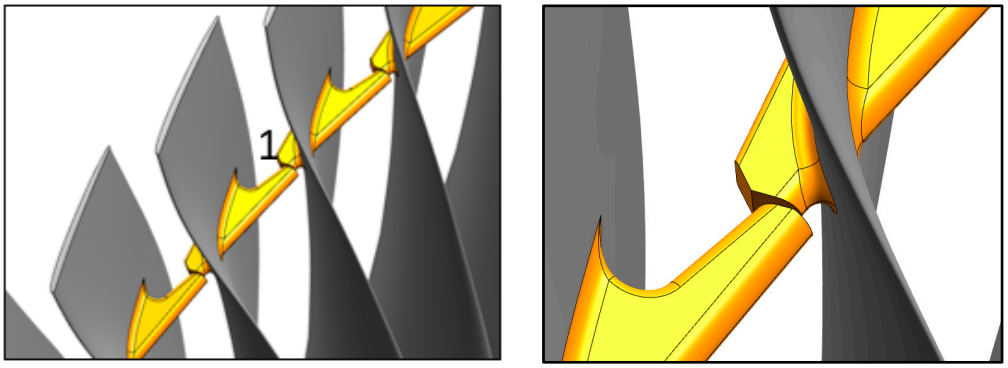

(**a**) (**b**)

Figure 19. (**a**) Portion of steam turbine. (**b**) Zoom on 1. Snubber contact surfaces between two adjacent blades.

Figure 19 depicts a portion of a real steam turbine in a unformed condition, which means that the geometry shown is in the configuration prior to the start-up of the machine. When the turbine is put into operation, the surfaces between two adjacent snubbers come into contact, which provides greater system stiffness.

The contact forces acting on these surfaces are not as high as those on the anchorage, which means that when the blade vibrates, relative motion or detachment can occur.

Considering what was discussed in the previous section, if there is detachment between two contact surfaces, intermittent contact can occur, so for modelling this phenomenon, a contact model that includes normal load variation is necessary.

For this purpose, when the blade model is meshed, every pair of contact nodes is coupled by the contact model shown in Figure 1, which is characterized by a tangential and a normal stiffness.

Figure 19 shows a portion of a bladed disk as an example of the typical context in which the considerations made in this paper can be exploited. For simplicity of calculation, the results shown below will still be on a system with 2 degrees of freedom but with system frequency values and contact parameter values typical of the blades of a real turbine.

Considering only one contact pair, the test case presented in Section 3 can be used to perform the non-linear forced response. Realistic contact parameters values are set for the calculations. The values of the contact parameters shown in Table 10 are chosen considering numerical analysis carried out in the literature on real bladed disks. In real turbine applications the number of contact pairs and the values of the corresponding contact parameter are usually chosen, when contact surfaces are stuck (without sliding), to obtain the same frequencies that would be obtained in Ansys under the same condition. To the authors' knowledge, it is recommended to choose the minimum values of contact parameters that guarantee the match of frequencies, in order to avoid convergence problems.

Table 10. Realistic contact parameters test case.

Parameter	Units	Value
M	Kg	1.6
K	$\frac{N}{mm}$	$8 * 10^5$
C	$\frac{N*s}{mm}$	0.4
K_t	$\frac{N}{mm}$	$5 * 10^5$
K_n	$\frac{N}{mm}$	$7 * 10^5$
F_0	N	100
μ	/	0.3
α	rad	$\frac{\pi}{4}$

Table 10 reports the test case parameters used to perform the calculations.
Two cases are considered:

- Case 1: The first computation is performed with a positive gap value of 0.3 mm and external forcing amplitude $F_0 = 100$ N.
- Case 2: The second computation is performed with a negative gap value of -0.2 mm and external forcing amplitude $F_0 = 100$ N.

The results obtained are shown in Figure 20:

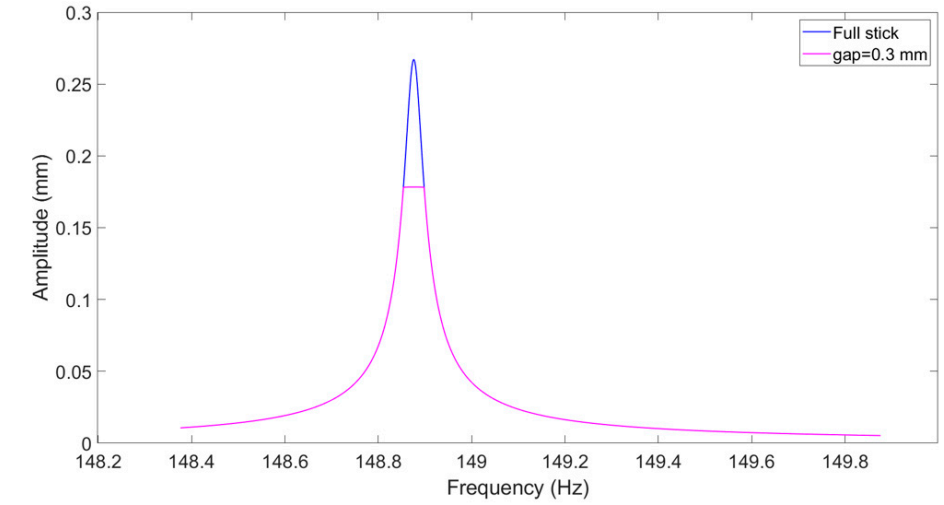

(**a**)

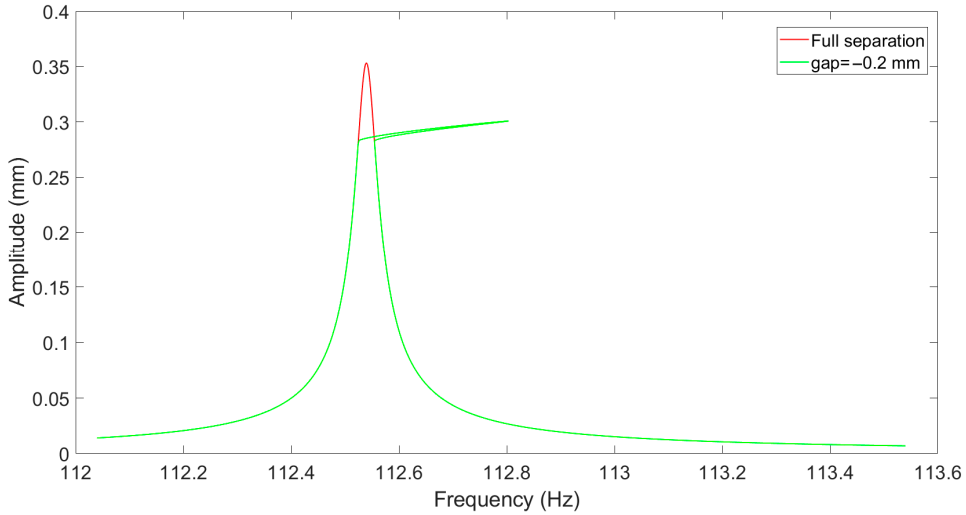

(**b**)

Figure 20. (**a**) Non-linear response with positive gap. (**b**) Non-linear response with negative gap.

With the used parameters chosen for performed calculation, the natural frequency of the system in full separation condition results as 112.53 Hz, while the natural frequency in full stick condition is 148.87 Hz, which are realistic values for the first bending mode of a last stage steam turbine blade. Computation times for both cases are reported in Table 11.

Table 11. Computation times.

Case	Computation Time	Units
1	6	s
2	635.9	s

From Figure 20a,b, the difference between the two calculations is clearly evident. In the case with a positive gap value, there is no intermittent contact, allowing the natural continuation scheme to converge successfully without the need for the arc length continuation method. This computation was carried out using 2^7 time samples per period.

The calculation with negative gap, instead, shows intermittent contact; therefore, the pseudo arc length continuation scheme is necessary to get around the turning point.

To ensure the solver convergence 2^{16} time samples per period were necessary in this case.

The obtained results confirm what was observed in the sensitivity analysis:

- When there is no intermittent contact, the forced non-linear response can be calculated with a natural continuation technique and with a limited number of time samples per period; this leads to a small computation time.
- When intermittent contact occurs, the pseudo arc length continuation technique is necessary to compute the non-linear FRF, and the number of time samples required to ensure solver convergence is larger, which leads to a higher but inevitable computation effort. The effect of the contact parameters, especially of the normal stiffness, is also appreciable; in fact, by comparing case 2 of this section with case 2 of Section 4.1 performed with 2^{12} time samples per period, a great difference in terms of calculation time can be seen. This is explained by the fact that in case 2 of this chapter, the contact parameters are orders of magnitude higher, which leads to the need to use more time samples to ensure the solver convergence.

6. Conclusions

The purpose of this paper is to provide guidelines for designers using non-linear calculation tools in the field of turbomachinery. A nonlinear solver requires certain parameters to be set. In this paper, the parameters that most affect convergence were analyzed.

The first parameter analyzed was the number of time samples needed to discretize the forces and displacements over a period. This parameter is the most critical, particularly when intermittent contact is present. An insufficient number of samples can prevent the solver from converging, even when considering only a single harmonic. Conversely, in the absence of intermittent contact, aliasing errors can be avoided with a relatively low number of samples per period. However, this number must still exceed the theoretical minimum associated with a given truncation order, since the nonlinear force in the time domain remains a non-smooth function even without contact loss.

The second parameter investigated was the harmonic truncation order, which represents the number of terms considered in the HBM equations. The sensitivity analysis revealed that, if intermittent contact occurs, this computation parameter must be set higher than one because the first harmonic component alone is insufficient to approximate the nonlinear force of the time signal. For the cases explored in this paper, a harmonic truncation order of five was enough to ensure the right FRF computation.

Regarding the situation in which there is no intermittent contact, beyond a certain value of samples per period one harmonic component may be enough to compute the right FRF, but it is always recommended to use a harmonic order truncation order of at least five to be sure to avoid computation issues.

The final parameters examined were the contact parameters, which define the tangential and normal forces computed within the contact model. The most significant finding is the strong dependence of the required number of time samples per period on the normal stiffness. Specifically, as the normal stiffness increases, more samples are needed to achieve convergence. This behavior can be attributed to the fact that higher normal stiffness results in greater normal forces, which in turn increase the likelihood of intermittent contact. In contrast, variations in tangential stiffness did not affect the number of samples required for convergence, which remained constant across all values explored.

Considering the outcome of the sensitivity analysis and what was discussed in previous sections, the guidelines for designers using non-linear tools in which are implemented the computation methods described in this paper can be summarized by the following points:

- When there is no intermittent contact, natural continuation ensures the solver convergence without issues, so in this case the pseudo arc length continuation technique is useless, only leading to higher computation effort. It is recommended to use a minimum harmonic order truncation of five, even if for some cases only the first harmonic might be enough.
- When intermittent contact occurs, turning points appear in the FRF curves, requiring the use of the pseudo arc length continuation technique to avoid convergence issues. Another crucial aspect is the oversampling of the time signal: in such cases, an insufficient number of time samples per period can lead to convergence failure, making the use of a high number of samples advisable. To the authors' knowledge, this parameter does not reach a clear plateau; therefore, no fixed optimal value can be defined, as it depends on the specific system and the contact parameters involved.
- When there is intermittent contact, increasing only the harmonic truncation order does not ensure the solver convergence, but you must also use a proper number of time samples per period; of course this leads to long, but inevitable, computation times.
- Increasing the normal stiffness value, higher values of time samples per period must be used to reach convergence. If possible, it is recommended to distribute the global normal stiffness on multiple contact pairs (the number depends mainly on the mesh of the model) to have lower stiffness values locally, and thus avoid using an excessive number of time samples per period, which increases computation times.

The results that come out from the sensitivity analysis performed in this paper are obtained considering a 2D contact model, which includes a variable normal force and a tangential friction force in one direction on the contact surface. These results can be easily extended to a 3D contact model where, instead of calculating the tangential force on the contact surface in a single direction, the tangential force is calculated in two perpendicular directions, but the calculation scheme remains the same.

Author Contributions: Numerical analysis, E.C.; Methodology, E.C.; Data curation, E.C.; Writing-original draft preparation, E.C.; Writing-review and editing, T.B. and D.B.; Supervision, A.B. All authors have read and agreed to the published version of the manuscript.

Funding: This publication was produced while attending the PhD programme in Mechanical Engineering at the Polytechnic of Turin, Cycle XXXVIII, with the support of a scholarship co-financed by the Ministerial Decree no. 352 of 9 April 2022, based on the NRRP—funded by the European Union—NextGenerationEU—Mission 4 "Education and Research", Component 2 "From Research to Business", Investment 3.3, and by the company Ansaldo Energia.

Data Availability Statement: The original contributions presented in this study are included in the article. Further inquiries can be directed to the corresponding author.

Conflicts of Interest: The authors declare no conflicts of interest.

Abbreviations

The following abbreviations are used in this manuscript:

HBM	Harmonic Balance Method
AFT	Alternating Frequency Time
PAC	Pseudo Arc Length Continuation
NC	Natural Continuation
ULS	Underlying Linear System
FFT	Fast Fourier Transform
IFFT	Inverse Fast Fourier Transform
FRF	Frequency Response Function
DOF	Degree Of Freedom
DOFs	Degrees Of Freedom
TS	Time Samples

References

1. Griffin, J.H. Friction Damping of Resonant Stresses in Gas Turbines Airfoils. *J. Eng. Power* **1980**, *102*, 329–333. [CrossRef]
2. Petrov, E.P. Explicit Finite Element Models of Friction Dampers in Forced Response Analysis of Bladed Disks. *J. Eng. Gas Turbines Power* **2008**, *130*, 022502. [CrossRef]
3. Ferhatoglu, E.; Gastaldi, C.; Botto, D.; Zucca, S. An Experimental and Computational Comparison of the Dynamic Response Variability in a Turbine Blade with Under-Platform Dampers. *Mech. Syst. Signal Process.* **2022**, *172*, 108987. [CrossRef]
4. Yang, B.D.; Chen, J.J.; Menq, C.H. Prediction of Resonant Response of Shrouded Blades with Three-Dimensional Shroud Constraint. *J. Eng. Gas Turbines Power* **1999**, *121*, 523–529. [CrossRef]
5. Yajie, S.; Jie, H.; Yingchun, S.; Zigen, Z. Forced Response Analysis of Shrouded Blades by an Alternating Frequency/Time Domain Method. In *Volume 5: Marine; Microturbines and Small Turbomachinery; Oil and Gas Applications; Structures and Dynamics, Parts A and B*; ASMEDC: Barcelona, Spain, 2006; pp. 865–872.
6. Szwedowicz, J.; Visser, R.; Sextro, W.; Masserey, P.A. On Nonlinear Forced Vibration of Shrouded Turbine Blades. *J. Turbomach.* **2008**, *130*, 011002. [CrossRef]
7. Gu, W.; Xu, Z.; Liu, Y. A Method to Predict the Nonlinear Vibratory Response of Bladed Disc System with Shrouded Dampers. *Proc. Inst. Mech. Eng. Part C J. Mech. Eng. Sci.* **2011**, *226*, 1620–1632. [CrossRef]
8. Yuan, J.; Gastaldi, C.; Denimal Goy, E.; Chouvion, B. Friction Damping for Turbomachinery: A Comprehensive Review of Modelling, Design Strategies, and Testing Capabilities. *Prog. Aerosp. Sci.* **2024**, *147*, 101018. [CrossRef]
9. Berruti, T.; Firrone, C.M.; Pizzolante, M.; Gola, M.M. Fatigue Damage Prevention on Turbine Blades: Study of Underplatform Damper Shape. *Key Eng. Mater.* **2007**, *347*, 159–164. [CrossRef]
10. Cardona, A.; Coune, T.; Lerusse, A. A Multi-Harmonic Method for Nonlinear Vibration Analysis. *J. Numer. Methods* **1998**, *217*, 1593–1608.
11. Sanliturk, K.Y.; Ewins, D.J. Modelling Two-Dimensional Friction Contact and Its Application Using Harmonic Balance Meth-Od. *J. Sound Vib.* **1996**, *193*, 511–523. [CrossRef]
12. Siewert, C.; Panning, L.; Wallaschek, J.; Richter, C. Multiharmonic Forced Response Analysis of a Turbine Blading Coupled by Nonlinear Contact Forces. *J. Sound Vib.* **2010**, *132*, 082501. [CrossRef]
13. Sun, H.; Zhang, D.; Wu, Y.; Shen, Q.; Hu, D. A Semi-Analytical Multi-Harmonic Balance Method on Full-3D Contact Model for Dynamic Analysis of Dry Friction Systems. *Chin. J. Aeronaut.* **2024**, *37*, 309–329. [CrossRef]
14. Yang, D.; Lu, Z.-R.; Liu, J.; Wang, L. Harmonic Balance Method Integrated with a Customized State-Space Algorithm for the Periodic Solutions of Structures with Frictional Hysteresis. *Nonlinear Dyn.* **2025**, *113*, 22747–22764. [CrossRef]

15. McGurk, M.; Yuan, J. Prediction and Validation of Aeroelastic Limit Cycle Oscillations Using Harmonic Balance Methods and Koopman Operator. *Nonlinear Dyn.* **2025**. [CrossRef]
16. Lin, R.; Hou, L.; Chen, Y.; Jin, Y.; Saeed, N.A.; Chen, Y. A Novel Adaptive Harmonic Balance Method with an Asymptotic Harmonic Selection. *Appl. Math. Mech.* **2023**, *44*, 1887–1910. [CrossRef]
17. Gao, Q.; Fan, Y.; Wu, Y.G.; Li, L.; Zhang, D.Y. Insight into the Influence of Frictional Heat on the Modal Characteristics and Interface Temperature of Frictionally Damped Turbine Blades. *J. Sound Vib.* **2024**, *581*, 118410. [CrossRef]
18. Botto, D.; Campagna, A.; Lavella, M.; Gola, M.M. Experimental and Numerical Investigation of Fretting Wear at High Temperature for Aeronautical Alloys. In *Proceedings of the ASME Turbo Expo 2010: Power for Land, Sea, and Air. Volume 6: Structures and Dynamics, Parts A and B*; ASME: Glasgow, UK, 2010. [CrossRef]
19. Gastaldi, C.; Grossi, E.; Berruti, T.M. On the Choice of Contact Parameters for the Forced Response Calculation of a Bladed Disk with Underplatform Dampers. *J. Glob. Power Propuls. Soc.* **2017**, *1*, 5D19RH. [CrossRef]
20. Firrone, C.M.; Allara, M.; Gola, M.M. A Contact Model for Nonlinear Forced Response Prediction of Turbine Blades: Calculation Techniques and Experimental Comparison. In *Proceedings of the Volume 5: Structures and Dynamics, Parts A and B*; ASMEDC: Berlin, Germany, 2008; pp. 573–582.
21. Woiwode, L.; Balaji, N.N.; Kappauf, J.; Tubita, F.; Guillot, L.; Vergez, C.; Cochelin, B.; Grolet, A.; Krack, M. Comparison of Two Algorithms for Harmonic Balance and Path Continuation. *Mech. Syst. Signal Process.* **2020**, *136*, 106503. [CrossRef]
22. Cameron, T.M.; Griffin, J.H. An Alternating Frequency/Time Domain Method for Calculating the Steady-State Response of Nonlinear Dynamic Systems. *J. Appl. Mech.* **1989**, *56*, 149–154. [CrossRef]
23. Chan, T.F.C.; Keller, H.B. Arc-Length Continuation and Multigrid Techniques for Nonlinear Elliptic Eigenvalue Problems. *SIAM J. Sci. Stat. Comput.* **1982**, *3*, 173–194. [CrossRef]
24. Yang, B.D.; Chu, M.L.; Menq, C.H. Stick-Slip Separation Analysis and Non-Linear Stiffness and Damping Characterization of Friction Contacts Having Variable Normal Load. *J. Sound Vib.* **1998**, *210*, 461–481. [CrossRef]
25. Petrov, E.P.; Ewins, D.J. Analytical Formulation of Friction Interface Elements for Analysis of Nonlinear Multi-Harmonic Vibrations of Bladed Disks. *J. Turbomach.* **2003**, *125*, 364–371. [CrossRef]
26. Raeen, K. A Study of the Gibbs Phenomenon in Fourier Series and Wavelets. Ph.D. Thesis, University of New Mexico, Albuquerque, NM, USA, 2008.